

Broadband Asymmetrically Fed Circularly Polarized Slot Antenna for Mid-Band 5G Smartphone Applications

Aniket Gunjal and Ujwala Kshirsagar*

Abstract—A compact asymmetrically fed U shape slot antenna for 5G smartphone application is presented. The antenna consists of two major components that are responsible for generating broadband circular polarization (CP) (i) the microstrip patch feed structure employed at the top plane and (ii) U shape slot mechanism employed at the ground plane. The U shape ground radiator is approximately half wavelength slot mode which is responsible for lower band CP operation. The planar monopole structure is formed by the microstrip line feed. This planar monopole is a quarter wavelength mode used for achieving higher band CP operation. By combining these two CP modes generated by U shape slot and port-line structure, a broadband CP antenna is designed. The circular polarization is achieved with lesser complexity in the design structure. To get the practical validation of the simulated design, it is then fabricated and tested for measured results without using power divider. The measured axial ratio bandwidth covers from 2.00 GHz to 6.50 GHz (4.50 GHz), and the -10 dB Impedance Bandwidth (IBW) covers from 1.66 GHz to 8.10 GHz (6.44 GHz) respectively. The isolation between two asymmetric port-lines is greater than 14.5 dB within 3-dB axial ratio bandwidth.

1. INTRODUCTION

Circularly polarized antennas are the most prominent antennas for today's wireless communication because of their advantages over linearly polarized antennas [1–3]. These antennas have the capability to compensate the multipath interference's and fading issues, and ultimately they mitigate the polarization loss problems [4]. Broadband antennas are required for high-speed data transmission and reception which enhances the quality of service in wireless communication [5, 6]. Slot antennas are very much suitable for broadband applications as these antennas have benefits like miniaturization in size, light weight, simple structure, and easy fabrication. Hence, these planar printed antennas are extensively used in several frequency bands of operation such as Global Positioning System (GPS), mobile Long Term Evolution (LTE), and surveillance radar systems. Generally, the dual feed type of CP Multi-Input Multi-Output (MIMO) antenna is used to achieve a good enhancement in 3-dB axial ratio bandwidth. These CP MIMO antennas are also used to improve the circular polarization diversity performance and polarization ratio of the antenna. Different shapes of slot structures are available in the existing literature that gives wideband CP operation. U shape slot antenna along with some perturbations or inclusion of parasitic elements in the shape of U structure gives broadband operation [7, 8]. Conventional antennas having narrower impedance bandwidth, which can be further improved by the slot mechanism and orthogonal feeding structures, give rise to broadband CP radiation. Various antennas have been used for broadband CP generation, which are studied in the literature such as microstrip line ground slot antennas [9], Substrate Integrated Waveguide (SIW) ground slot antennas [10], planar monopole slot antennas [11], spiral slot antennas [12], and corner truncated slot antennas [13, 14]. Semi-arc shaped radiating strip lines are placed orthogonally to achieve easy circular polarization. The mutual coupling

Received 18 August 2021, Accepted 13 September 2021, Scheduled 27 September 2021

* Corresponding author: Ujwala Kshirsagar (ujwala.kshirsagar@sitpune.edu.in).

The authors are with the Symbiosis Institute of Technology, Symbiosis International (Deemed University), Pune, India.

effect between two feed lines is mainly reduced by introducing a narrow strip in the ground circular slot structure, which ultimately improves isolation amongst the feeding elements. Two vertical and two horizontal square strips are protruded in the outer surface of a ground circular slot to enhance return loss bandwidth and peak gain of antenna [15]. A simple planar monopole antenna with hexagonal shaped patch and protruded L strips improves axial ratio bandwidth (ARBW) of antenna [16] to obtain ARBW of 5.06 GHz. The square ring slot antenna with orthogonal T structure feed-lines creates CP waves. The axial ratio bandwidth can be further enhanced by inserting an inverted L shape strip placed at the left corner of patch with additional smaller length microstrips to get axial ratio bandwidth of 1.7 GHz [17]. The composite feed aperture coupled antenna having corner truncated patch is used to obtain circular polarization. An I-shaped ground slot is used to improve isolation between two orthogonal ports, and C-shaped ground slot is used to improve the ARBW of antenna. The antenna is tested without using a power divider, which shows more than 18 dB of inter-port isolation level between two orthogonal ports [18]. Dual-polarized CP MIMO antennas can satisfy the need for good polarization diversity required in some wireless applications.

In this manuscript, a broadband circularly polarized antenna having circular radiation pattern is presented. By adjusting the patch length, width, and ground slot shape, it is possible to enhance the gain and axial ratio bandwidth. The radiation pattern shows good CP performance in both xz plane and yz plane. The proposed MIMO antenna array with a common ground structure is advantageous as it is very easy to integrate with other devices because of the common ground structure, and the another advantage of this common ground slot MIMO antenna is that it reduces the mutual coupling behavior between the antenna elements which ultimately improves the isolation level.

The organization of this manuscript follows. The introduction about the dual-feed type of CP slot antennas is provided in Section 1. A detailed explanation about the proposed antenna structure is shown in Section 2. MIMO antenna performance analysis is in Section 3 and the parametric result analysis in Section 4. The simulated and measured results are compared in Section 5, and finally, the manuscript is concluded in Section 6.

2. PROPOSED GEOMETRY OF CP ANTENNA

Figure 1 depicts the top view of dual-feed circularly polarized antenna geometry. The antenna is fabricated using square-shaped FR4 (Flame-Retardant) substrate material having $\epsilon_r = 4.4$ and $\tan\delta = 0.027$. The length, width, and thickness of the antenna are $48 \times 48 \times 1$ mm here. The antenna has dual-feed microstrip line ports (Port1, port2), a U shape slot with some perturbations, and a metallic ground structure. The microstrip lines are connected to the Q shape patch which creates a patch feed type of network. This patch feed network is used to excite bottom ground U shape slot. The shape of

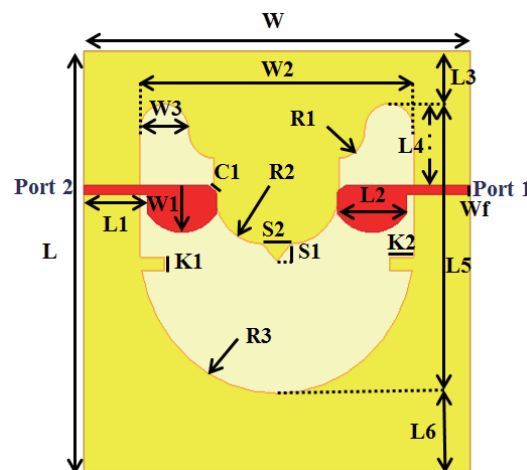


Figure 1. Top view of proposed CP antenna geometry.

the patch is selected in such a way that it improves the surface vector current distribution of antenna at the higher frequency bands. The Q shape patches improves 3-dB axial ratio bandwidth at higher frequency bands. These types of feeding structures are also advantageous for obtaining lower value of ECC. The circular polarization is obtained by achieving two orthogonal electric line field vectors having the same magnitude with 90° phase difference between them. This U structure ground slot is used to achieve a wider bandwidth. This ground U slot radiator is a half-wavelength structure that provides one CP resonance in lower frequency side, and another CP resonance on higher frequency side is achieved through an asymmetric dual-feed port-line antenna structure. If port 1 is excited, it gives Left Hand Circular Polarization (LHCP) wave, and if port 2 is excited, it radiates Right Hand Circular Polarization (RHCP) waves. If we excite one port, then another port is considered as matched terminated to 50Ω impedance of the antenna. The antenna shows good symmetry in the design structure whenever you see it from either left side view or right side view of the antenna. It means that if one takes a vertical cut of antenna from middle, picks the left side part, and then put in front of mirror, it will show right hand side view of antenna showing design symmetry. This CP antenna is simulated with the help of High-Frequency Structure Simulator (HFSS) 19.0 software. The antenna simulation results show 1.99–8.20 GHz (6.21 GHz) of impedance bandwidth, peak isolation of -23 dB within the ARBW, and 1.93–6.29 GHz (4.36 GHz) of axial ratio bandwidth as shown in Fig. 2. The amplitude ratio is close to 0 dB at some frequencies within the axial ratio bandwidth, and phase difference nearly 90° within the axial ratio bandwidth is achieved. The axial ratio curve is very close to the 0 dB level at 3.8 GHz & 6.0 GHz. Perfect 90° of phase difference at this frequency is obtained, and the amplitude ratio curve is close to 0 dB level at this frequency. The optimized parameter values for the proposed fabricated structure are as follows:- $L = 48$, $W = 48$, $L1 = 8.0$, $L2 = 8.5$, $L3 = 6.0$, $L4 = 9.3$, $L5 = 33.0$, $L6 = 9.0$, $W1 = 5.3$, $W2 = 34.0$, $W3 = 6.0$, $C1 = 1.2$, $R1 = 3.2$, $R2 = 6.0$, $R3 = 17.0$, $K1 = 1.5$, $K2 = 3.0$, $Wf = 1.0$, $S1 = 2.0$, and $S2 = 3.5$ (unit = mm).

3. MIMO ANTENNA PERFORMANCE ANALYSIS

The MIMO antenna performance is calculated with the help of parameters such as envelope correlation coefficient (ECC), polarization ratio, channel capacity loss (CCL), total active reflection coefficient (TARC), and diversity gain (DG). Every parameter having its acceptable limit such as CCL and ECC considered to be as small as possible. Generally, ECC & CCL values should be smaller than 0.5. TARC value should be below the -10 dB level. The acceptable limit for diversity gain is near 10 dB.

3.1. Orthogonal Polarization Diversity of Antenna

Envelope Correlation Coefficient (ECC) is an prominence factor for evaluating orthogonal polarization diversity of circularly polarized MIMO antenna. This antenna is verified for its orthogonal polarization diversity performance by using an ECC parameter. In general, to get good circular polarization diversity performance, ECC parameter is considered to be as minimum as possible. ECC formula is derived from S -parameters of antenna shown in Equation (1). The benefit of this approach is to understand the mutual coupling effect between two asymmetrically fed resonator lines and input impedance matching effect which gives a clear idea on polarization diversity performance of antenna.

ECC parameter is calculated by using the following equation,

$$\rho_e = \frac{|S_{11}^* S_{12} + S_{21}^* S_{22}|^2}{(1 - (|S_{11}|^2 + |S_{21}|^2))(1 - (|S_{22}|^2 + |S_{12}|^2))} \quad (1)$$

where,

S_{11} = input reflection coefficient which represents how much energy reflected from antenna

S_{12} = power reflected from port 2 to port 1

S_{21} = power reflected from port 1 to port 2 and

S_{22} = output reflection coefficient of antenna in multi feed type of networks.

Figure 3 shows the simulated and measured values of ECC. As shown in Fig. 3, the ECC value is less than 0.01 within the axial ratio bandwidth of antenna. It shows that the realized antenna has good polarization diversity.

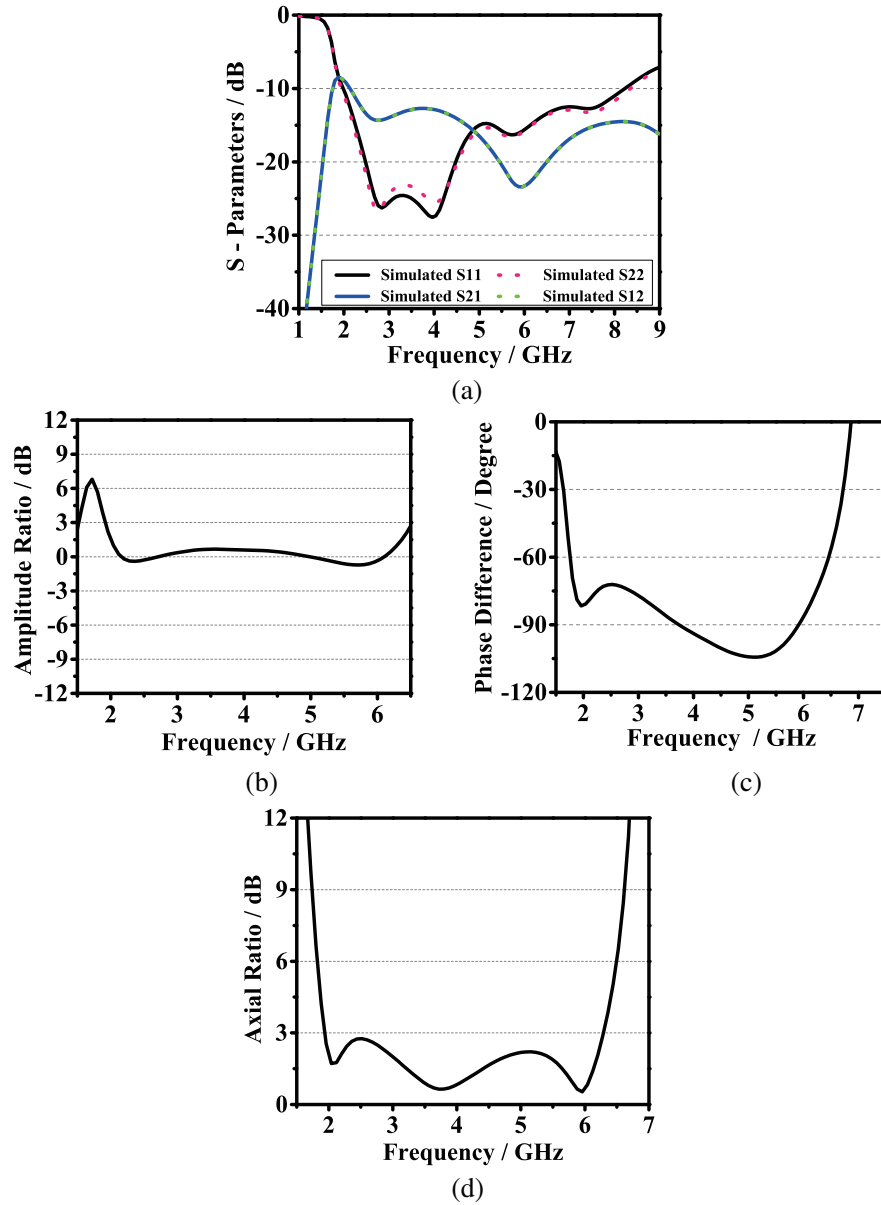


Figure 2. Simulated (a) S -parameters, (b) amplitude ratio, (c) phase difference and (d) axial ratio bandwidth.

3.2. Polarization Ratio of Antenna

The polarization purity is verified through the polarization ratio of that antenna. Fig. 3 illustrates the antenna's polarization purity. The magnitude of LHCP leads to the magnitude of RHCP, and hence LHCP antenna is designed. Therefore, because of the design symmetry in antenna structure, the two polarizations seem equal in magnitude, but they are opposite in direction with each other. As the axial ratio curve moves downward towards 0 dB level, it will improve the polarization ratio of antenna. As shown in Fig. 2, the axial ratio curve is very close to the 0 dB level at 3.8 GHz and 6.0 GHz frequency. The polarization ratio of antenna at 3.8 GHz & 6.0 GHz frequencies is high almost 30 dB. The minimum value of polarization level is 10 dB by considering the operational CP bandwidth as shown in Fig. 3.

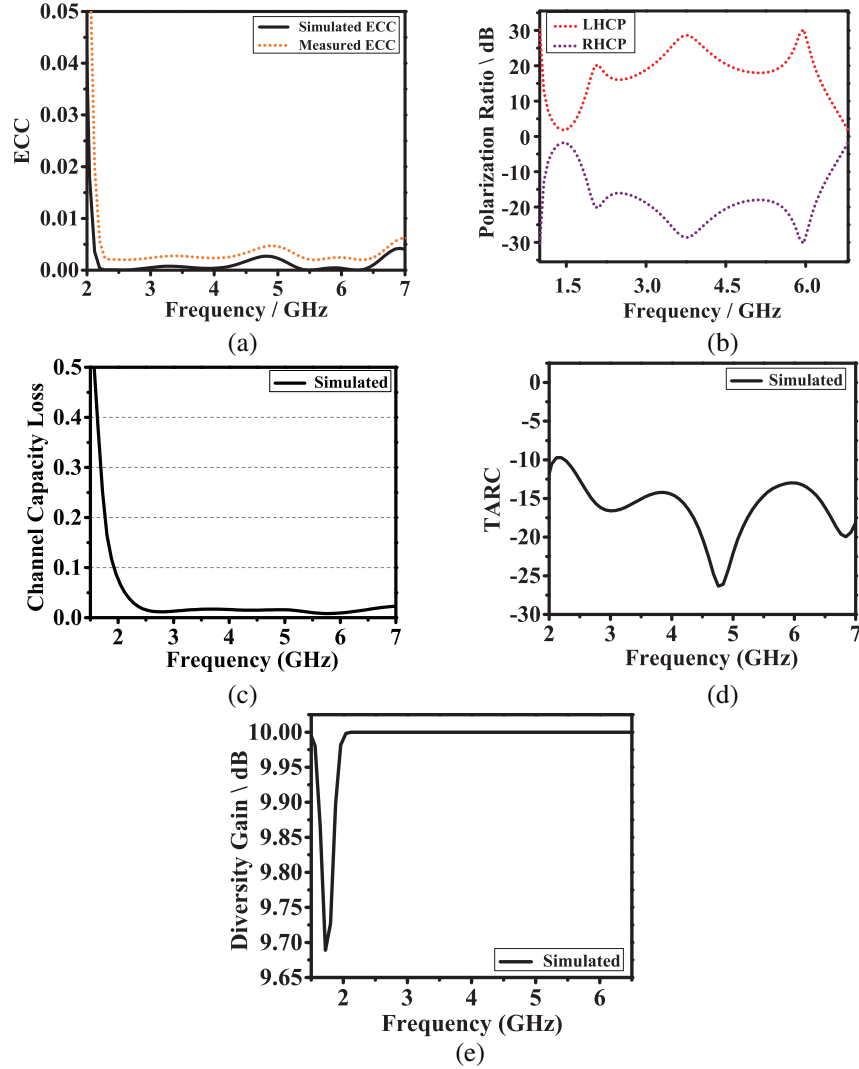


Figure 3. Simulated (a) Envelope Correlation Coefficient, (b) Polarization Ratio, (c) Channel Capacity Loss, (d) TARC and (e) Diversity Gain of proposed antenna.

3.3. Channel Capacity Loss (CCL)

Channel capacity loss is also the prominent factor which is calculated using S -parameters of the MIMO antenna. The simulated value of channel capacity loss is less than 0.1. The CCL is expressed by the formula given below in Equation (2).

$$CCL = -\log_2 \det(\psi^R) \tag{2}$$

where,

$$\psi^R = \begin{bmatrix} p_{11} & p_{12} \\ p_{21} & p_{22} \end{bmatrix} \tag{3}$$

$$p_{ii} = 1 - (|S_{ii}|^2 + |S_{ij}|^2), p_{ij} = -(S_{ii}^* S_{ij} + S_{ji}^* S_{ij}) \text{ for } i, j = 1, 2.$$

3.4. Total Active Reflection Coefficient (TARC)

The total active reflection coefficient (TARC) parameter is used to incorporate the overall effect of all antennas employed in a MIMO structure. TARC is formulated by using Equation (4). The TARC value

is less than -10 dB within the operational bandwidth of antenna.

$$TARC = -\sqrt{\frac{(S_{mm} + S_{mn}^2) + (S_{nm} + S_{nn})^2}{2}} \quad (4)$$

3.5. Diversity Gain (DG)

Diversity gain parameter is used to find the signal to interference ratio of MIMO antenna. Diversity gain is obtained by first finding the calculated value of ECC of the MIMO antenna. The relation between the two parameters is found by the following Equation (5). For the lower value of ECC, the diversity gain is higher. The diversity gain of more than 9.90 dB is observed for the whole operating CP bandwidth of MIMO antenna.

$$DG = 10\sqrt{1 - (ECC)^2} \quad (5)$$

The proposed MIMO antenna performance is verified through these five important parameters. The above five parameter values are within the acceptable limits prescribed above. CCL is smaller than 0.1, and a small value of ECC is obtained which is below 0.01 level. TARC shows combined impedance matching effect of all antennas in MIMO system. The minimum TARC value of -10 dB is obtained. The diversity gain near 10 dB level is obtained. Thus, from the achieved simulated values of ECC, polarization ratio, CCL, TARC, and DG, it has been concluded that the proposed broadband smartphone antenna satisfies the trustworthy MIMO performance.

4. PARAMETRIC RESULT ANALYSIS

The parametric analysis is carried out to verify its impact on various antenna parameters such as impedance bandwidth, isolation, and ARBW. In the following parametric optimization study, the length-width of rectangular ground strip protruded on either side of U slot and triangular ground strip protruded on the middle portion of the grounded U slot is changed to verify its impact on impedance bandwidth, isolation, and ARBW of antenna. Axial ratio bandwidth is easily controlled by optimizing the rectangular ground strip and triangular ground strip. The impedance bandwidth and axial ratio bandwidth improvement is done with the help of two rectangular strips inserted in the opposite side of the U slot and a triangular strip inserted at the middle portion of the ground U slot. These rectangular strips have a significant impact on the surface vector current distribution of the antenna. The vertical current and horizontal current moving on the outer contour surface of ground U slot are modified due to the insertion of both rectangular and triangular strips which will give rise to betterment in impedance bandwidth as well as 3-dB axial ratio bandwidth.

4.1. Length-Width Effect of Two Rectangular Ground Strips

The effect of change in length-width of rectangular ground strip on impedance bandwidth, isolation, and ARBW is depicted in Fig. 4. It shows that as length-width of rectangular strip increases the impedance bandwidth shifts at the higher frequencies. Conversely, as the length-width of the rectangular strip increases the isolation at the higher band is decreased. It can also be seen that there is no effect on the lower frequency side of isolation. The U shape slot is a half wavelength slot mode which is mainly responsible for lower frequency characteristics, and patch feed network is a quarter wavelength structure which is mainly responsible for higher frequency characteristics.

The length-width of rectangular strip is adjusted such that it improves axial ratio bandwidth of antenna at lower frequency side and also impedance bandwidth on higher frequency side. The length of 1.5 mm and width of 3 mm are taken to get improvement in ARBW at lower frequency and impedance bandwidth at higher frequency. Too narrow and too wide length-width of the rectangular ground strip has no such good effect on the lower frequency side of ARBW, and it shows poor performance at the lower frequency.

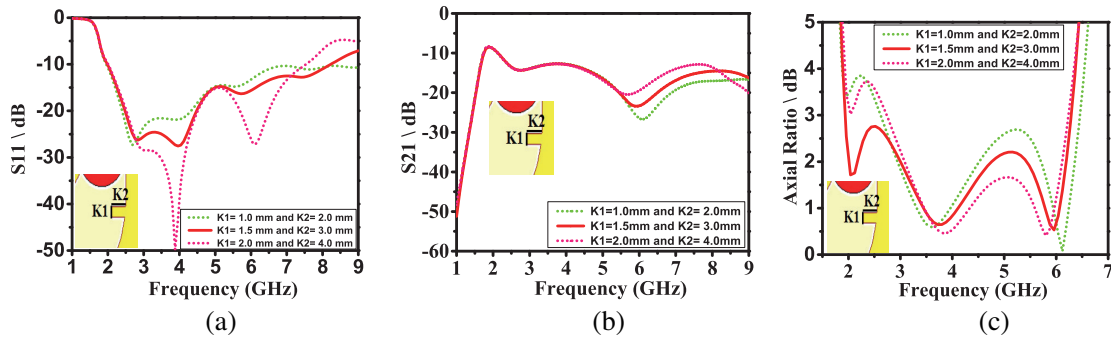


Figure 4. Effect of rectangular strip on (a) IBW, (b) isolation and (c) ARBW.

4.2. Length-Width Effect of Middle Triangular Ground Strip

The length-width variation effect of triangular ground strip on the performance of antenna in terms of impedance bandwidth, isolation, and ARBW is depicted in Fig. 5. It can be observed that the triangular ground strip has no major impact on impedance bandwidth and isolation values of the proposed antenna. Mainly, the triangular ground strip affects the 3-dB axial ratio bandwidth. It shows that as the length-width of triangular strip increases the operating band shifts at the higher frequency side of ARBW. The optimum values of length 2.0 mm and width of 3.5 mm are selected to get slight improvement in the wider axial ratio bandwidth at the lower as well as higher frequency band.

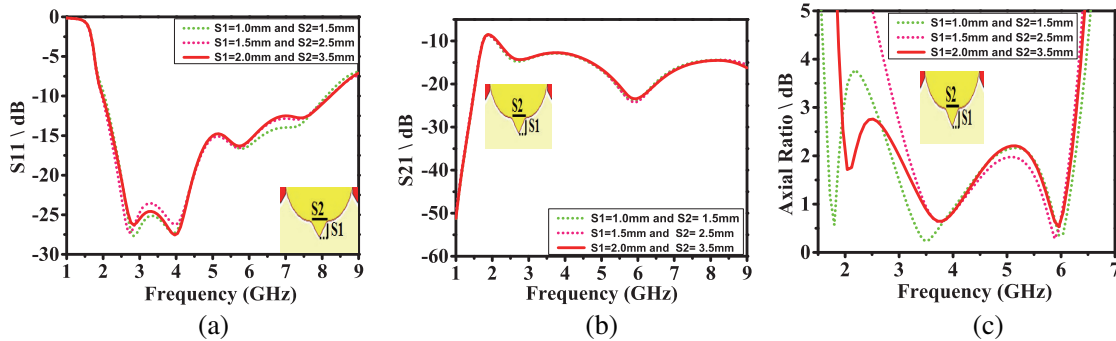


Figure 5. Effect of triangular strip on (a) IBW, (b) isolation and (c) ARBW.

5. EXPERIMENTAL RESULT ANALYSIS OF THE FABRICATED DESIGN

Fig. 6 shows the simulated and measured graphs for S_{11} , S_{21} , ARBW, gain, and radiation efficiency. The antenna is tested using an anechoic chamber for radiation efficiency, 3-dB axial ratio bandwidth, and radiation pattern measurement, and all other measurements are taken with the help of Agilent technologies RF-VNA (Radio Frequency Vector Network Analyser) having model No.-N9925A. The experimental setup contains a probe (Horn) antenna placed at the left side in Fig. 8 which is used because the standard horn antenna with a known gain is suitable for measured result analysis of the fabricated antenna under test. The fabricated antenna which is under test is placed in front of the horn antenna using a positioner. The use of that positioner is to have rotational control in azimuth and elevation angles. The anechoic chamber contains pyramidal shape absorbing material. It is used for absorbing unwanted electromagnetic radiation from outside sources so that the measurement analysis is carried out without the effect of other interfering sources.

The horn antenna is taken as a reference antenna to evaluate the performance of CP antenna which is depicted in Fig. 8. The horn antenna is placed at a distance of 1 meter from the CP antenna which is under test in anechoic chamber. To verify the practical reliability and accuracy of simulated

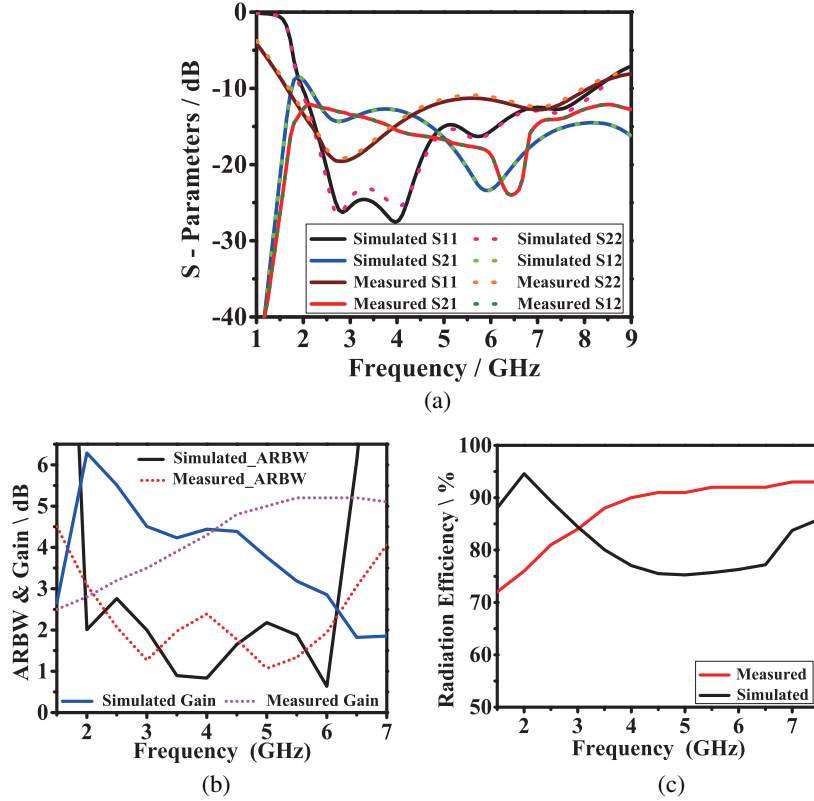


Figure 6. Comparison between the simulated and measured (a) S-Parameters (b) axial ratio bandwidth, gain and (c) radiation efficiency.

design, it is fabricated using an FR4 dielectric substrate. Fig. 8 shows the top side view and bottom ground side view of the proposed fabricated dual-feed antenna structure. The simulated graph for return loss covers a broader range of 1.99–8.20 GHz while the measured graph shows improvement in -10 dB return loss bandwidth from 1.66 to 8.10 GHz. The measured isolation graph shows better isolation in lower frequency side than simulated results. The simulated ARBW is about 4.36 GHz which ranges from 1.93 GHz to 6.29 GHz. The measured ARBW shifts to 210 MHz in the higher frequency band in comparison with simulated ARBW. The measured 3-dB axial ratio bandwidth is slightly higher than simulated axial ratio bandwidth. The measured 3-dB axial ratio bandwidth is about 4.5 GHz which is ranges from 2.0 GHz to 6.5 GHz. In comparison with simulated gain, measured gain is different showing peak gain of 5.2 dB at 5.5 GHz frequency in higher frequency band within 3-dB ARBW. The simulated peak gain of antenna is 6.29 dB at the 2.0 GHz frequency in lower frequency band within 3-dB ARBW. Similarly, simulated and measured antenna radiation efficiencies also differ. Measured radiation efficiency shows more than 75% of efficiency within the whole ARBW. The antenna radiation efficiency showing near 100% efficiency in simulation which is practically impossible to obtain. So it is plotted using \tanh function instead of using abs function to fit it into the graph. Also, due to the antenna's manufacturing tolerances, some measurement errors, and bad soldering effects on feedline structure, the simulated and measured radiation efficiencies differ. This is the main reason that the simulated and measured radiation efficiency plots are different. The antenna's gain is the product of radiation efficiency and directivity of antenna. Similarly, the measured and simulated gains also differ. In general, the patch feed network forms a quarter wavelength structure that gives an improvement in the higher frequency band of the CP antenna. The patch cut of 1 mm on either side of both the patches has a significant effect on the gain over a higher frequency band. Hence, the measured results show more correctness than the simulated results of gain and radiation efficiency.

The radiation pattern depicted in Fig. 7 shows a deviation in gain from broadside direction at 4 GHz and 6 GHz which is the major reason that the measured peak antenna gain at lower band is lower than

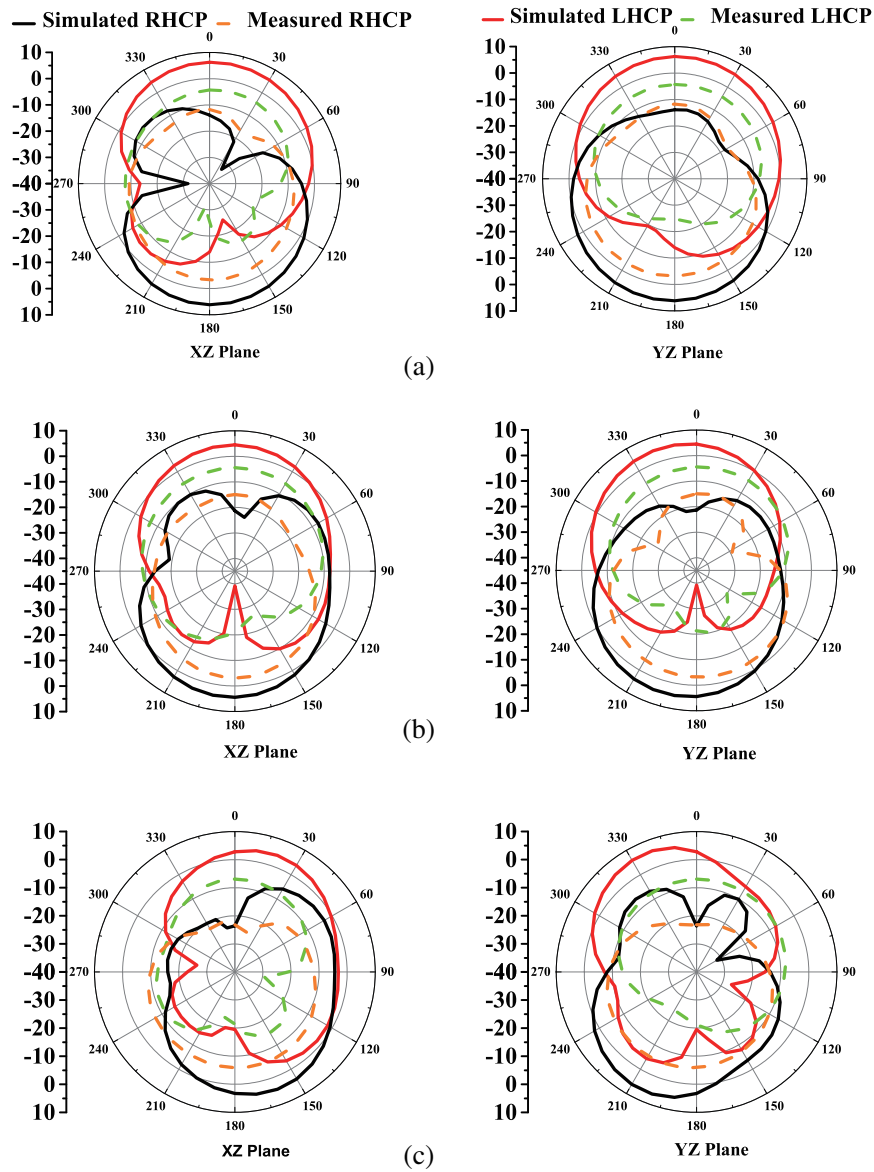


Figure 7. Simulated and measured radiation pattern for port 1 (a) 2 GHz (b) 4 GHz (c) 6 GHz.

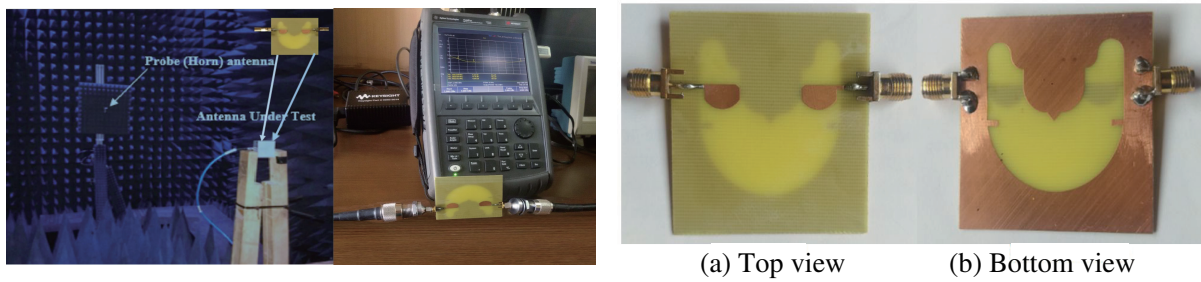


Figure 8. (I) Anechoic chamber test environment & VNA measurements and (II) Fabricated (a) top view & (b) bottom view of CP antenna.

upper band. The cross-polarization between RHCP and LHCP components is better than 13.0, 15.0, and 24.0 dB, respectively for both the planes. In comparison with the measured and simulated results of radiation plots, the measured LHCP and RHCP plots capture smaller areas in the radiation pattern plot than that of the simulated radiation pattern plots. The radiating area of antenna at the ground surface area which is responsible for lower band CP operation is larger than the radiating area of the top patch structure which is responsible for the upper band CP operation. the 3-dB beamwidths of antenna at 2.0 GHz in xz and yz planes are 95.56° and 102.37° , respectively. Similarly, the 3-dB beamwidths of antenna at 4.0 GHz in xz and yz planes are 73.75° and 73.38° , respectively. Also, 3-dB beamwidths of antenna at 6 GHz are 61.56° and 53.45° in xz and yz planes. The MIMO structures are extensively used to obtain different levels of polarizations which ultimately improves the total coverage area in MIMO environments. The orthogonal arrangement of feedline with all possible CP senses enhances the transmission and reception capability of MIMO antenna. The LHCP and RHCP polarizations have polarization symmetry in both the xz and yz planes at 2 GHz, 4 GHz, and 6 GHz frequency because of the symmetry in antenna design structure. The LHCP component lies in the $+z$ direction, and RHCP component lies in the $-z$ direction indicating leading LHCP performance when port 1 is excited. RHCP component lies in the $+z$ direction, and LHCP component lies in the $-z$ direction indicating leading RHCP performance if we excite port 2. Table 1 shows the comparison of various CP antennas available in the existing literature along with the proposed work. The comparison table is made to show the advantages of the proposed antenna in terms of size, IBW, ARBW, and gain parameters. The comparison table describes the proposed dual-feed slot antenna having miniaturization in size, broader impedance bandwidth, and high peak gain within the wider axial ratio bandwidth.

Table 1. Comparison of various circularly polarized antennas.

Size (mm)	IBW (GHz)	Isolation (dB)	ARBW (GHz)	Peak Gain (dB)	Ref.
120×65×1.60	3.30–5.00, 1.70	> 18.8	—	4.7	[19]
70×70×1.52	2.40–2.77, 0.37, & 4.96–5.64, 0.68	> 21.0	—	3.9 & 4.1	[20]
32×32×1.60	1.54–2.08, 0.54 & 3.96–8.40, 4.42	—	3.80–8.22, 4.22	1.6 & 4.1	[21]
50×50×1.60	3.40–3.80, 0.40	> 12.0	—	4.2	[22]
34×34×1.44	3.52–3.58, 0.06 & 5.00–5.24, 0.24	> 21.0 & 19.0	3.52–3.58, 0.06	1.5 & 2.2	[23]
120×120×30	2.70–3.10, 0.40	—	2.15–2.93, 0.78	—	[24]
19.5×36×1.60	2.50–6.50, 4.00	—	3.10–6.20, 3.10	3.4	[25]
120×65×0.8	1.35–2.75, 1.40	13.4	1.47–2.55, 1.08	3.5	[26]
100×50×1.6	1.80–4.00, 2.20	13.0	—	4.5	[27]
40×30×1.6	3.20–5.85, 2.65	17.5	—	3.5	[28]
48×48×1.00	1.66–8.10, 6.44	> 14.5	2.00–6.50, 4.50	5.2	Prop.

6. CONCLUSION

The dual feed ground slot MIMO antenna having broadband circular polarization is proposed. The feed width and feed position have major impact on impedance bandwidth. By protruding two rectangular strips and one triangular strip in the U shape ground slot, it is also possible to have enhancement in return loss bandwidth and 3-dB axial ratio bandwidth. A smaller cut of 1.2 mm on the top side of both the patches gives improvement in gain. The radiation pattern shows good CP performance for different operating frequencies. A Q shape patch is used to give a wider impedance bandwidth. The shape of the patch is adjusted such that it gives an improvement in axial ratio bandwidth of antenna. Measured peak gain of proposed antenna is 5.2 dB at 5.5 GHz frequency. The gain varies from 2.8 to 5.2 dB showing better gain stability within the axial ratio bandwidth. Thus, this dual feed CP antenna having broader impedance bandwidth, enhanced gain, and wider axial ratio bandwidth is achieved. The proposed dual feed MIMO antenna enhances the polarization diversity performance, and the MIMO antenna having high throughput capability for faster data rate communication makes it suitable for mid-band 5G smartphone applications.

REFERENCES

1. Wang, K., X. Liang, W. Zhu, J. Geng, J. Li, Z. Ding, and R. Jin, "A dual wideband dual polarized aperture shared patch antenna with high isolation," *IEEE Antennas and Wireless Propagation Letters*, Vol. 17, No. 5, 735–738, 2018.
2. Sze, J. Y., C. I. Hsu, Z. W. Chen, and C. C. Chang, "Broadband CPW fed circularly polarized square slot antenna with lightning shaped feedline and inverted L grounded strips," *IEEE Transactions on Antennas and Propagation*, Vol. 58, No. 3, 973–977, 2009.
3. Liu, Y. W. and P. Hsu, "Broadband circularly polarised square slot antenna fed by coplanar waveguide," *Electronics letters*, Vol. 49, No. 16, 976–977, 2013.
4. Gao, S. S., Q. Luo, and F. Zhu, *Circularly Polarized Antennas*, John Wiley & Sons, 2013.
5. Murch, R. D. and K. B. Letaief, "Antenna systems for broadband wireless access," *IEEE Communications Magazine*, Vol. 40, No. 4, 76–83, 2002.
6. Shokri, M., V. Rafii, S. Karamzadeh, Z. Amiri, and B. Virdee, "Miniaturised ultra wideband circularly polarised antenna with modified ground plane," *Electronics letters*, Vol. 50, No. 24, 1786–1788, 2014.
7. Xu, R., J. Y. Li, J. Liu, S. G. Zhou, Z. J. Xing, and K. Wei, "A design of dual wideband planar printed antenna for circular polarization diversity by combining slot and monopole modes," *IEEE Transactions on Antennas and Propagation*, Vol. 66, No. 8, 4326–4331, 2018.
8. Gunjal, A. and S. Kumar, "Gain enhancement in U slotted broadband dual circularly polarized antenna for s band radar applications," *International Conference on Emerging Smart Computing and Informatics (ESCI)*, 124–128, 2020.
9. Chen, W. J., H. H. Chen, C. H. Lee, and C. I. G. Hsu, "Differentially fed wideband circularly polarized slot antenna," *IEEE Transactions on Antennas and Propagation*, Vol. 67, No. 3, 1941–1945, 2018.
10. Li, Y., Z. N. Chen, X. Qing, Z. Zhang, J. Xu, and Z. Feng, "Axial ratio bandwidth enhancement of 60 GHz substrate integrated waveguide fed circularly polarized LTCC antenna array," *IEEE Transactions on Antennas and Propagation*, Vol. 60, No. 10, 4619–4626, 2012.
11. Kumar, T. and A. R. Harish, "Broadband circularly polarized printed slot monopole antenna," *IEEE Antennas and Wireless Propagation Letters*, Vol. 12, 1531–1534, 2013.
12. Siahcheshm, A., J. Nourinia, C. Ghobadi, M. Karamirad, and B. Mohammadi, "A broadband circularly polarized cavity backed Archimedean spiral array antenna for C band applications," *AEU—International Journal of Electronics and Communications*, Vol. 81, 218–226, 2017.
13. Rahimi, M., M. Maleki, M. Soltani, A. S. Arezomand, and F. B. Zarrabi, "Wide band SRR inspired slot antenna with circular polarization for wireless application," *AEU — International Journal of Electronics and Communications*, Vol. 70, No. 9, 1199–1204, 2016.
14. Wu, Z., G. M. Wei, X. Li, and L. Yang, "A single-layer and compact circularly polarized wideband slot antenna based on "bent feed"," *Progress In Electromagnetics Research*, Vol. 72, 39–44, 2018.
15. Parchin, N. O., H. J. Basherlou, Y. I. A. Al-Yasir, A. A. S. Alabdullah, and R. A. Abd-Alhameed, "Ultra wideband diversity MIMO antenna system for future mobile handsets," *Sensors*, Vol. 20, No. 8, 2371, 2020.
16. Chandu, D. S. and S. S. Karthikeyan, "A novel broadband dual circularly polarized microstrip fed monopole antenna," *IEEE Transactions on Antennas and Propagation*, Vol. 65, No. 3, 1410–1415, 2017.
17. Saini, R. K. and S. Dwari, "A broadband dual circularly polarized square slot antenna," *IEEE Transactions on Antennas and Propagation*, Vol. 64, No. 1, 290–294, 2015.
18. Chakrabarti, S., "Composite feed dual circularly polarized microstrip antenna with improved characteristics," *Microwave and Optical Technology Letters*, Vol. 58, No. 2, 283–289, 2016.
19. Biswas, A. and V. R. Gupta, "Design and development of low profile MIMO antenna for 5G new radio smartphone applications," *Wireless Personal Communications*, Vol. 111, No. 3, 1695–1706, 2020.

20. Malviya, L., R. K. Panigrahi, and M. V. Kartikeyan, "A 2×2 dual band MIMO antenna with polarization diversity for wireless applications," *Progress In Electromagnetics Research*, Vol. 61, 91–103, 2016.
21. Midya, M., S. Bhattacharjee, G. K. Das, and M. Mitra, "Dual band dual polarized compact planar monopole antenna for wide axial ratio bandwidth application," *International Journal of RF and Microwave Computer Aided Engineering*, Vol. 30, No. 5, e22152, 2020.
22. Saxena, S., B. K. Kanaujia, S. Dwari, S. Kumar, and R. Tiwari, "MIMO antenna with built-in circular shaped isolator for sub 6 GHz 5G applications," *Electronics Letters*, Vol. 54, No. 8, 478–480, 2018.
23. Islam, S. N. and S. Das, "Dual band CPW fed MIMO antenna with polarization diversity and improved gain," *International Journal of RF and Microwave Computer Aided Engineering*, Vol. 30, No. 4, e22128, 2020.
24. Wen, L., S. Gao, Q. Luo, W. Hu, and B. Sanz-Izquierdo, "Design of a broadband circularly polarized antenna by using axial ratio contour," *IEEE Antennas and Wireless Propagation Letters*, Vol. 19, No. 12, 2487–2491, 2020.
25. Ellis, M. S., A. R. Ahmed, J. J. Kponyo, J. Nourinia, C. Ghobadi, and B. Mohammadi, "Simple circularly polarized planar monopole inverted T shaped antenna," *Microwave and Optical Technology Letters*, Vol. 62, No. 1, 405–410, 2020.
26. Chaudhary, P., A. Kumar, and A. Yadav, "Pattern diversity MIMO 4G and 5G wideband circularly polarized antenna with integrated LTE band for mobile handset," *Progress In Electromagnetics Research M*, Vol. 89, 111–120, 2020.
27. Akdagli, A. and A. Toktas, "Design of wideband orthogonal MIMO antenna with improved correlation using a parasitic element for mobile handsets," *International Journal of Microwave and Wireless Technologies*, Vol. 8, No. 1, 109–115, 2016.
28. Kulkarni, J., A. Desai, and C. Y. D. Sim, "Wideband four-port MIMO antenna array with high isolation for future wireless systems," *AEU-International Journal of Electronics and Communications*, Vol. 128, 153507, 2021.